Higgs boson discovery through top-partners decays using jet substructure

Graham D. Kribs, Adam Martin, and Tuhin S. Roy

Higgs Discovery through Top-Partners using Jet Substructure

Graham D. Kribs,[1, 2] Adam Martin,[1] and Tuhin S. Roy[3]

[1] *Theoretical Physics Department, Fermilab, Batavia, IL 60510*
[2] *Department of Physics, University of Oregon, Eugene, OR 97403*
[3] *Department of Physics, University of Washington, Seattle, WA 98195*

Top-partners – vector-like quarks which mix predominantly with the top quark – are simple extensions of the standard model present in many theories of new physics such as little Higgs models, topcolor models, and extra dimensions. Through renormalizable mixing with the top quark, these top-partners inherit couplings to the Higgs boson. Higgs bosons produced from the decay of top-partners are often highly boosted and ideal candidates for analyses based on jet substructure. Using substructure methods, we show that light Higgs bosons decaying to $\bar{b}b$ can be discovered at the 14 TeV LHC with less than 10 fb^{-1} for top-partner masses up to 1 TeV.

I. INTRODUCTION

While the fermions of the standard model (SM) are notoriously chiral, extensions of the SM often involve new fermions whose left and right-handed components have the same quantum numbers, so-called vector-like fermions. Because of this charge assignment, vector-like fermions do not require electroweak symmetry breaking to have mass, making them a particularly self-contained, worry free extension of the SM. The interactions between new vector-like fermions and the matter in the SM depend on the quantum numbers of the new fermions. One common choice is to include new fermions with the same quantum numbers as the right-handed quarks and which mix predominantly with the top quark: a top-partner. The restriction to mixing with the top quark is driven in part by necessity – the interactions of lighter fermions are more tightly constrained by experiment – and in part by the idea that the large mass of the top is an indication that it is more intimately connected with new ultraviolet physics. Despite their vector-like nature, these top-partners do interact with the Higgs boson because of mass mixing. The goal of this paper is to demonstrate that this coupling between vector-like top-partners and the Higgs boson can have profound impact on the discovery potential of a light Higgs boson at the LHC.

While certainly phenomenologically interesting, extending the SM with a vector-like top-partner is also well-motivated from a theoretical perspective. In order to maintain a naturally light Higgs boson, divergent quantum corrections from loops of top quarks must be removed. One way to reduce the top-induced divergence is to enlarge the approximate global symmetries of SM, which requires new particles, including top-partners. In little Higgs theories [1–14], the top-loop divergence is canceled precisely by a loop of a vector-like top-partner with exactly the properties described above. Some of the models are sufficiently safe from electroweak precision constraints [15–18] to allow these vector-like top-partners to be accessible at the LHC [19–22]. Vector-like quarks are also prevalent in extra-dimensional models [23–26] as the Kaluza-Klein (KK) excitations of SM fermions, in top-color models [27], in supersymmetric little higgs models [28–35] and even in the simplest extensions of the SM where gauge coupling unification serves as the only guiding principle besides a WIMP dark matter, e.g. [36].

Collider studies of vector-like top-partners are plentiful [19–22, 37–45]. However, past searches focus on the discovery of the top-partners, rather than using the top-partners to enhance the discovery of *other* particles. Direct collider searches put a lower bound of $\sim$ few hundred GeV on the mass of the top-partners [43, 44]. New colored particles can be copiously produced at the LHC, and through the top-partner–Higgs interaction, top-partner decays will generate a new source of Higgs bosons. A new production mode of Higgs bosons is most interesting when Higgs boson is light (namely, $m_h \lesssim 130$ GeV). In this mass range, the Higgs boson requires over 10 fb^{-1} to find in one of the more traditional SM searches, such as $h \to \tau^+\tau^-$ and $h \to \gamma\gamma$, and over 30 fb^{-1} to find in the $h \to \bar{b}b$ channel using jet substructure techniques [46].

One complication in this scenario is that top-partners tend to interact with, and therefore, decay primarily to the third generation quarks. So, while the decay of top-partners does occasionally yield Higgs bosons, the decay products of the Higgs bosons are surrounded by a sea of top and bottom quarks. The large number of bottom quarks is especially problematic since it introduces a large combinatoric impediment to Higgs reconstruction via the dominant $h \to \bar{b}b$ mode.

In this paper we look for *boosted* light Higgs bosons that decay through the $h \to \bar{b}b$ mode. Boosted Higgs boson decay to $b\bar{b}$ can be captured by looking for jet with substructure consistent with massive particle decay. The shift to large jets and boosted objects has several advantages: (i) the high mass, distinct substructure, and heavy flavor content within the large jets are all effective handles which can be used to separate the signal from the background [46–61]; and (ii) by capturing the Higgs boson entirely within a single jet we can reduce the combinatorial problem – only b-jets which are close enough to be encompassed by a single fat jet are used for resonance reconstruction.

Previous attempts have shown that the Higgs boson can be discovered spectacularly well in the supersymmetric extension of the SM using jet substructure techniques

even from a sample of 10 fb^{-1} of data [62, 63]. What sets this work apart is the fact that unlike weak scale supersymmetry, the final states consist solely of SM particles and hence do not automatically have large missing energies. Without a clean sample of new physics events, finding Higgs resonance is more challenging. We propose a strategy that combines various boosted object taggers (such as top and W/Z taggers) with conventional cuts and requirements. We find that for top-partners up to about 800 GeV, the algorithm is capable of discovering the Higgs boson in the $b\bar{b}$ channel with high significance before any SM search.

The setup of this paper is the following: In Sec. II we describe the minimal vector-like top-partner model and define the mass eigenstates and couplings. Next, in Sec. III we describe the analysis strategy – the tools, both conventional and unconventional that we will use, the flow of analysis cuts. In Sec. IV we give further simulation details and present our results. Following our main results, we provide two example models whose low energy effective theory contains the exact states and interactions necessary for our study (Sec. V). We then conclude in Sec. VI with a discussion.

II. MIXING TOP-PARTNERS WITH THE TOP

While there are many possible vector-like extensions of the SM, in this work we will focus on the vector-like top. We enlarge the SM by two Weyl fermions: $T \equiv (3,1)_{\frac{2}{3}}$, $T^c \equiv (\bar{3},1)_{-\frac{2}{3}}$. With these quantum numbers, the simplest, renormalizable interactions we can write down involving the new fermions are:

$$\mathcal{L} \supset y_1 Q_3 H t^c + \delta\, T t^c + M T T^c, \qquad (1)$$

where Q_3 is the (SM) third generation electroweak doublet (t, b). Note that an additional term $Q_3 H T^c$ is also allowed under all symmetries. It can, however, be eliminated by rotating t^c and T^c and consequently redefining δ and M.

The mass eigenstates are combinations of the quarks t^c and T^c. The full mass matrix, including nonzero Higgs vacuum expectation value (vev) is given by

$$(t \; T) \begin{pmatrix} m & 0 \\ \delta & M \end{pmatrix} \begin{pmatrix} t^c \\ T^c \end{pmatrix}, \qquad (2)$$

where $m = \frac{y_1}{\sqrt{2}} v$ and v is the Higgs vev. In general, this mass matrix is not symmetric and can be diagonalized by a bi-unitary transformation which rotates the left handed and the right handed quarks by different angles. Under such a rotation, the quark mass eigenstates are related to the quarks in Eq. (1) in the following way

$$\begin{pmatrix} t_1 \\ t_2 \end{pmatrix} = \begin{pmatrix} \cos\theta_l & -\sin\theta_l \\ \sin\theta_l & \cos\theta_l \end{pmatrix} \begin{pmatrix} t \\ T \end{pmatrix}$$
$$\begin{pmatrix} t_1^c \\ t_2^c \end{pmatrix} = \begin{pmatrix} \cos\theta_r & -\sin\theta_r \\ \sin\theta_r & \cos\theta_r \end{pmatrix} \begin{pmatrix} t^c \\ T^c \end{pmatrix}. \qquad (3)$$

The angles θ_l, θ_r and the mass eigenvalues can be determined to be

$$\theta_l = \frac{1}{2}\tan^{-1}\left(\frac{2\,\delta\,m}{M^2 - m^2 + \delta^2}\right)$$
$$\theta_r = \frac{1}{2}\tan^{-1}\left(\frac{2\,\delta\,M}{M^2 - m^2 - \delta^2}\right) \qquad (4)$$
$$m_t = \cos\theta_l \cos\theta_r \, (m + \delta\,\tan\theta_l + M\,\tan\theta_l\tan\theta_r)$$
$$m_T = \cos\theta_l \cos\theta_r \, (M - \delta\,\tan\theta_r + m\,\tan\theta_l\tan\theta_r)$$

In a more useful parametrization, the angles and the couplings may be expressed as a function of m_t, m_T and $\eta = \delta/M$.

$$\tan\theta_r = \frac{m_T}{m_t}\tan\theta_l \qquad (5)$$

$$\theta_l = \frac{1}{2}\sin^{-1}\left(\eta\frac{2m_t m_T}{m_T^2 - m_t^2}\right) \qquad (6)$$

In order to study the collider phenomenology of this minimal setup we introduce four component Dirac spinors $t_D = \begin{pmatrix} t_1 \\ t_1^{c\dagger} \end{pmatrix}$ and $T_D = \begin{pmatrix} t_2 \\ t_2^{c\dagger} \end{pmatrix}$. The non-diagonal interactions of heavy top can then be recast in the form

$$\mathcal{L} \supset \frac{m_t \cos^2\theta_l}{v} h \, \bar{T}_D(\tan\theta_r \, P_L + \tan\theta_l \, P_R)\, t_D$$
$$+ \frac{g_2 \sin\theta_l \cos\theta_l}{2\cos\theta_W} Z_\mu \left(\bar{T}_D\gamma^\mu P_L t_D + \bar{t}_D\gamma^\mu P_L T_D\right) \qquad (7)$$
$$+ \frac{g_2 \sin\theta_l}{\sqrt{2}} \left(W_\mu^+ \bar{T}_D\gamma^\mu P_L b_D + W_\mu^- \bar{b}_D\gamma^\mu P_L T_D\right),$$

where $P_{L,R}$ are the usual projectors.

Within the minimal model, the top-partner can only decay to the Higgs boson, W or Z. In the limit of infinite T mass, the branching fractions for these modes are essentially governed by "Goldstone equivalence": T can only decay into Higgs degrees of freedom via the first term in Eq. (1) – two of these degrees of freedom are eaten to become the longitudinal polarization of $W^\pm$, one is eaten by the Z, and the remaining one is the physical Higgs boson. Therefore, we have:

$$BR(T \to t + h) \sim 25\%, \quad BR(T \to t + Z) \sim 25\%$$
$$BR(T \to b + W) \sim 50\%. \qquad (8)$$

Different kinematics among the three modes alters this ratio, especially for lighter m_T, however it remains a decent approximation [64]. To demonstrate this, we plot the branching fraction to the three modes as a function of m_T in Fig. 1.

III. BOOSTED HIGGS BOSONS FROM TOP-PARTNERS

A. Pair production versus single production of top-partners

Because of the T-b-W coupling in Eq. (7), single production of T is possible. However, the cross section
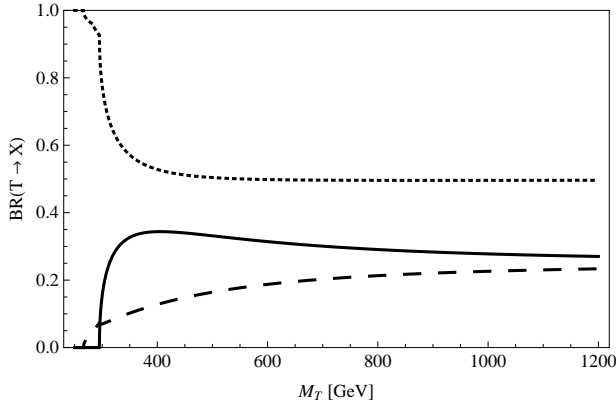
FIG. 1. Branching fraction of T to $t + h$, $m_h = 120$ GeV (solid), $b + W$ (dotted) and $t + Z$ (dashed) as a function of m_T. An η value of 0.5 has been chosen, though the branching ratios are essentially independent of η.
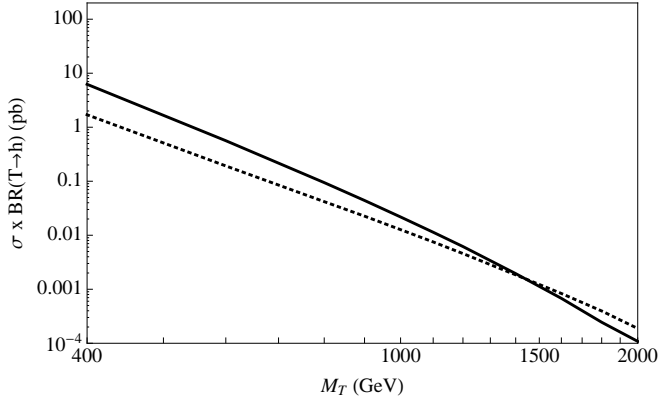

FIG. 2. Comparison of the production cross sections $\sigma(pp \to T\bar{T})$ (solid) and $\sigma(pp \to T+j, \bar{T}+j)$ (dotted) with at least one $T \to th$ at a 14 TeV LHC. The η parameter, which enters into single production, has been set to $1/2$. Smaller η decreases the cross section slightly.

depends on the b-quark pdf of proton, proportional to the electroweak coupling, and additionally suppressed because of W exchange in the $T-$channel. As long as $m_T \lesssim 1.1$ TeV, single production is always subdominant with respect to the QCD pair production of T [20, 37]. The dominance of the pair production below 1.1 TeV is demonstrated in Fig. 2.

Single production, while subdominant, does nevertheless create a cleaner final state compared to pair production, for example $pp \to T+q$. Cleaner states are certainly easier to reconstruct, however one T resonance in the event obviously provides fewer handles for distinguishing signal and background compared to T pair production. We find the cleaner final state does not compensate sufficiently for the lack of handles, so single production is always inferior to pair production, at least for the purpose of Higgs discovery. Therefore, in this work we concentrate on the following set of topologies: pair production of T followed by the decay of one T to $t+h$ and the other
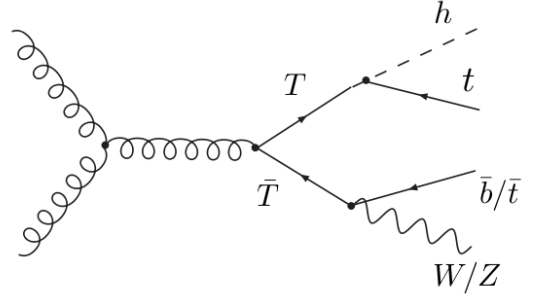

FIG. 3. A sample Feynman diagram for $T\bar{T}$ pair production followed by decays to a Higgs boson and a W or Z.

T to $b + W$ or $t + Z$.

B. Search Strategy

In order to come up with a successful search strategy, we first need to understand the standard model backgrounds as well as new physics backgrounds that we must overcome. Every interesting signal event contains multiple resonances, meaning Higgs bosons, W, Z, or tops. More specifically, in addition to the Higgs boson, there is always at least one top quark, one gauge boson and one b quark. Signal W bosons and b quarks can either come directly from the decay of the top-partner, or they can come from the decay of the top. The dominant SM backgrounds are $\bar{t}t+$jets, $\bar{t}t+\bar{b}b$ and $W/Z+$jets – all processes with large cross section containing gauge bosons and multiple hard jets. We will restrict our search to final states which contain at least one lepton to avoid an overwhelming QCD multi-jet background. The specifics of the backgrounds, including cross sections and generator details, will be given in Sec. IV.

The success of our search for a boosted Higgs boson relies crucially on combinations of conventional handles (such as existence of isolated leptons and large H_T *i.e.* scalar sum of visible energies in an event) and slightly unconventional tools (boosted object taggers). Each of these handles is described in more detail in the following subsection.

- **isolated lepton:** In our simulation leptons are considered as isolated if they have $p_T > 15$ GeV, $|\eta| < 2.5$ and if the energy deposited by hadrons within a cone of size $R = 0.4$ surrounding the lepton is less than 20% of the energy deposited by the lepton. Our simple implementation tags leptons with a 90% efficiency.

- **H_T:** H_T is defined as the scalar sum of all visible energy in the detector with $|\eta| < 4.0$. We calculate it by summing up the energies of all particles except neutrinos. Also note that after the hadrons are granularized into calorimeter cells, we disregard all

cells with energy less than 1 GeV and so these do not contribute to our estimation of H_T in an event.

- **top-tagger:** Top taggers are designed to find a hadronic top when it is boosted enough so that its decay products lie in one single jet. Examples of top taggers can be found in various recent works [48, 50, 51, 54, 55, 65, 66]. We employ the top-tagger introduced in Ref. [55] as it has been demonstrated to work significantly better with lower boost [67] and in particularly complex environments. In a sample of $t\bar{t}h$ events the tagger is found to have identified top with 43% efficiency and with 5% mistag rate when used on a sample of W + jets. Following [55], the inputs to the top-tagger are jets of size $R = 1.5$ which have been clustered with the Cambridge/Aachen algorithm [68–70]. The details of the declustering and subjet identification procedures can be found in Ref. [55].

- W/Z **tagger:** Like the top-tagger, the W/Z tagger also identifies hadronic and boosted W/Z. We use a modified version of an algorithm used by Butterworth et. al. (BDRS) [46] to find boosted Higgs bosons. The tagger consists of two parts: First, a jet is checked whether it contains both the partons from the decay of a massive particle going through a two body decay (*i.e.* the mass of the subjets are significantly smaller than the mass of the jet and the splitting of the jet into the two subjets is not too "asymmetric"). Jets which pass this criteria are "filtered " and retained if the mass of the filtered jet is within $(65 - 95)$ GeV. We use Cambridge/Aachen jets but with smaller size (namely, $R = 1.2$) as inputs to the W/Z tagger. We use the same declustering parameters as BDRS, however we *do not* require the subjets to carry heavy flavor. We find high-p_T W/Z events are tagged with $\sim 80\%$ efficiency, while QCD jets with $p_T \gtrsim 200$ GeV are misidentified as W/Z roughly $\sim 10\%$ of the time. The resulting tagged jet mass distribution, when the tagger works on W/Z samples and for QCD-jets, is shown below in Fig. 4. As expected, the QCD mistagged jets do not show any profile of a resonance in their jetmass distribution.

- **Higgs tagger:** The methodology of our Higgs tagger is identical to the BDRS algorithm as described in Ref. [46]. The tagger processes all tagged b-jets of size $R = 1.2$ clustered with the Cambridge/Aachen algorithm. The output of the tagger is a distribution of the jet substructure resonance mass, which contains both candidate Higgs bosons as well as backgrounds (from SM and new physics). In this paper we present these distributions, as well as an estimated signal significance of Higgs discovery given a peak and mass window. The full "Higgs
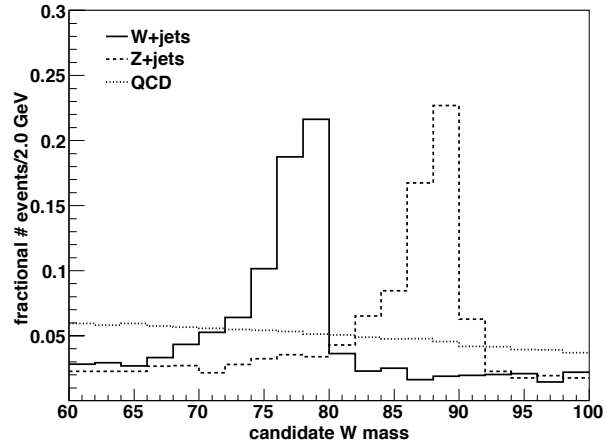

FIG. 4. Area normalized distribution of the jet mass for the W/Z-tagged jets when the tagger works on W + jets, Z + jets and QCD dijet samples.

tagger" is thus both extracting the distribution and specifying the candidate resonance jet mass window. Any boosted massive particle that decays to $\bar{b}b$ is identified, and thus very good resolution of the candidate resonance jet mass observable is critical. Heavy-flavor identification is an essential ingredient for picking out particles that are consistent with Higgs bosons. Encouraged by the results of the study in Ref. [55, 71], our simulations assume a flat 70% id efficiency for single b-tag with 1% fake rate [1].

Given that top-partner pair production results in purely SM final states that are generically boosted, our search strategy has been optimized precisely to find the boosted fraction of the signal. The boost distribution of the Higgs boson from the cascade decay of a top-partner is shown in Fig. 5. The Higgs boson p_T peaks at roughly $m_T/2$, which means a large fraction of the events containing a Higgs boson are boosted for *all* of the T masses considered in this paper. The boosted jet substructure techniques are particularly useful to separate the Higgs

---

[1] In this work we have neglected any difference in fake rate between charm-jets and light jets. However, it is important to stress that we actually tag each Higgs candidate *three* times; one tag to select the jet for BDRS tagging, then two more tags on BDRS subjets. We assume a flat 60%/2% tag/mistag rate outside of subjets and at 70%/1% tag/mistag rate for subjets. Therefore, an event with two b-jets is accepted $(0.6) \times (0.7)^2\%$ of the time; 0.6 for the initial flavor tag and $(0.7)^2$ for the two subjet tags. The fake rate can be anywhere from $(0.02) \times (0.01)^2$ for an event with zero b-jets to $0.6 \times 0.7 \times 0.01$ for an event with a single b that trips both the initial tag and one subjet tag. Note that, had we chosen to only tag the subjets but assumed an efficiency of 55% and fake rate of 0.17%, we would arrive at the same net tag/mistag rates.
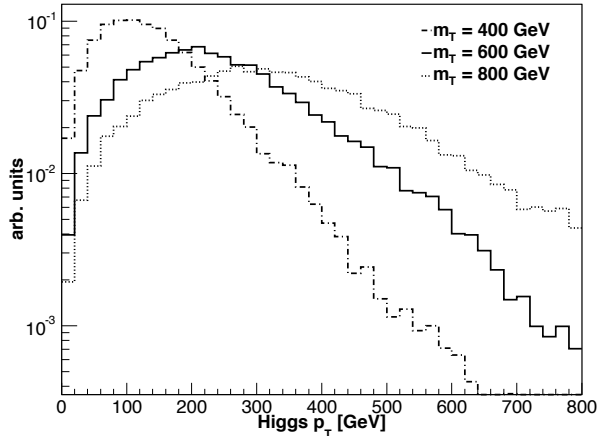
FIG. 5. Plot of the Higgs boson p_T in T decay for three different T masses.

boson decay to b-jets from b-jets that result from either decay of t or T. Additional cuts on moderate/large H_T and isolated lepton(s) further improves the signal significance.

As explained before, the Higgs tagger finds b-jets (would-be candidates for Higgs boson), but we employ it only after an input event passes through a series of selection criteria. We designed the criteria to capture all distinct signal topologies, rather than focusing on a subset. The different topologies are carefully chosen such that no event can be double-counted. In Fig. 6 all the channels of the selection procedure are depicted in a flow chart which we will briefly walk through now:

1. The top tagger runs on an input event and the event is classified in terms of the number of tops it identifies. All the cells contained within tagged tops are removed from the event.

2. The event is then further classified according to the number of isolated leptons present.

3. Events with large top and/or lepton multiplicities – in particular, events with a single top + more that one lepton or two tops + at least one lepton – have little standard model contamination. We select these events immediately as long as they contain at least one additional b-jet on which the Higgs tagger can be run.

4. Zero top + a single lepton is the most contaminated channel. To extract a good signal/background we employ additional requirements: the W/Z tagger finds at least one W/Z and it contains at least two b-jets, one of which contains a Higgs boson candidate. The additional W/Z requirement and the extra b-tag are necessary to bring $W/Z+$ jets under control.

5. For the rest of the channels, with one top + one lepton or no top + two (or more) leptons we demand that there be at least one b-jet.

After an event gets selected, the Higgs tagger runs over all leftover b-jets to determine whether these contain two b-tagged subjets consistent with the two-body decay of a Higgs boson. Once a Higgs-tagged jet is identified, we plot the jet mass. A peak in the signal events, above the Z mass but below where $h \rightarrow WW$ dominates, provides the evidence for a resonance consistent with a Higgs boson.

Having outlined our analysis strategy, we now present the details of our signal and background simulations and summarize our results.

IV. SIMULATION DETAILS AND RESULTS

To simulate the T pair production we use Madgraph and Madevent [72, 73]. The production cross sections are given in Table I.

m_T	$\sigma(pp \rightarrow T\bar{T})$
400 GeV	12.7 pb
600 GeV	1.29 pb
800 GeV	0.229 pb
1 TeV	0.054 pb

TABLE I. T pair production cross section at a $\sqrt{s} = 14$ TeV center of mass LHC at NLO with MCFM.

The heavy quark pair are subsequently decayed, showered and finally hadronized by PYTHIAv6.4 [74]. For the signal events, we also use the ATLAS tune [75] in PYTHIA to model the underlying event. For the background, events are simulated at parton level using ALPGENv13 [76], then similarly showered and hadronized using PYTHIA.

We do not use any realistic detector simulation or smearing in this work. The PYTHIA output events are directly used as input to our analysis. In each event, isolated leptons (we neglect the possibility of jets faking leptons here), isolated photons, and neutrinos (invisible to the detector) are identified while the rest of the particles (out to $|\eta| \leq 4$) are granularized into calorimeter 'cells' of size 0.1×0.1 in (η, ϕ). The three-momentum of each scale is rescaled so that the cell is massless, and all cells of energy less than 1 GeV are removed. The surviving cells are fed into the analysis chain described in Sec. III B above. Jet clustering is done using the inclusive Cambridge/Aachen algorithm, as implemented in Fastjet [77].

Once the events have been processed in the various channels, the final step in the Higgs search is to plot the Higgs candidate jet mass for all passing events and look for a feature. This can be done for each of the channels defined in Fig. 6 or by summing all channels
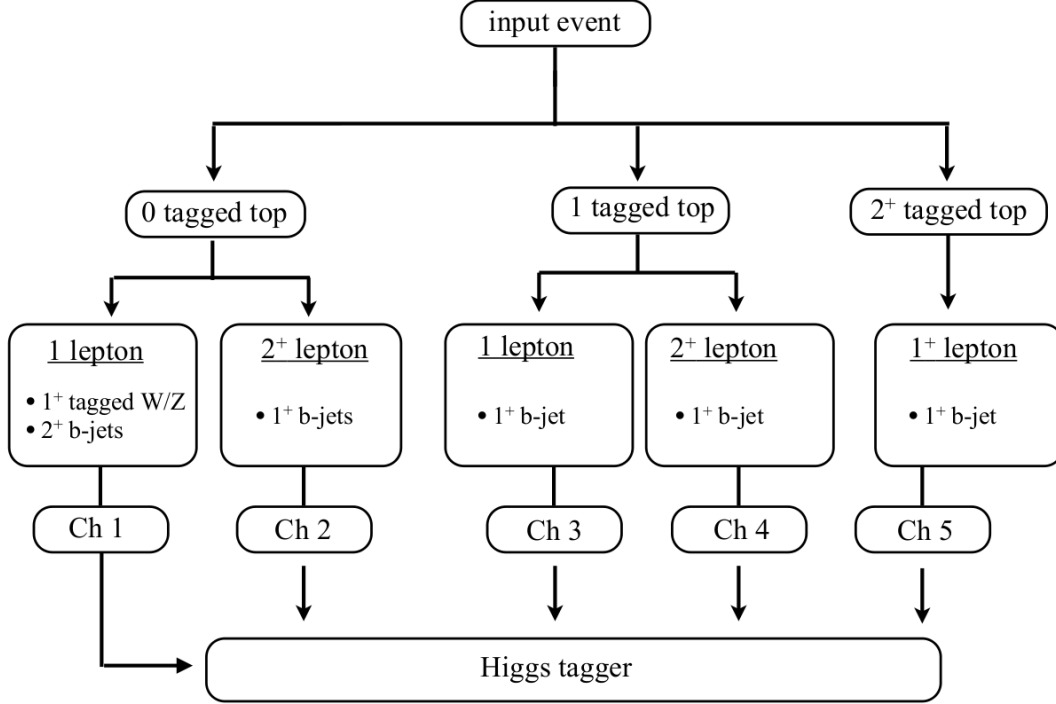
FIG. 6. Flow diagram to summarize our selection procedure. The flow has been devised so that no event can be counted more than once. In the figure, 1^+ means one or more objects are required. Additional cuts on $H_T > 1, 1.3$ TeV are imposed for top-partner masses of $800, 1000$ GeV respectively.

together. The invariant mass of the Higgs candidates summed across all channels for $m_T = 400, 600, 800$ and 1000 GeV are shown below in Fig. 7.

The peak in jet mass, consistent with Higgs decay, rises prominently above the background in all four examples. The new physics events to the left of the Higgs peak come predominantly from hadronically decaying Z [2]. According to the branching ratios in Eq. (8), equal amounts of Higgs bosons and Z are produced in T decay, however the branching fraction of $Z \to \bar{b}b$ is $\simeq 0.15$, so the Z feature is small. Hadronic W are also produced in T decay, however the majority of them are removed by cuts preceding the Higgs-tagger.

The measure we use for how well a particular analysis or sub-channel performs is the significance, which we define simply as $S/\sqrt{B}$. In addition to the SM background, we also include the new physics background – hadronically decaying, Z from T decay mentioned above. To account for this new physics background we define the total background to be the average of the number of events in the bins ± 2 from the putative Higgs peak. This is a crude, and somewhat conservative estimate for the significance. The significance in each channel, as well as the significance of all channels combined is summarized below in Table II.

	400 GeV		600 GeV		800 GeV		1 TeV	
	$S/\sqrt{B}$	S/B	$S/\sqrt{B}$	S/B	$S/\sqrt{B}$	S/B	$S/\sqrt{B}$	S/B
Ch 1	2.0	0.4	4.3	1.3	2.0	1.0	**	**
Ch 2	4.3	0.5	5.2	0.9	2.5	1.2	**	**
Ch 3	*	*	6.6	2.2	2.7	1.2	2.0	1.6
Ch 4	2.7	0.7	4.4	1.8	**	**	**	**
Ch 5	*	*	4.1	1.1	3.1	1.2	1.4	0.8
sum	5.2	0.5	10.5	1.2	5.2	1.2	2.4	1.2

TABLE II. The $S/\sqrt{B}$ and S/B obtained for the various search channels (using the Higgs peak ± 2 bins), as well as for the summed significance of all channels. The search was done for the heavy quark mass of 400 GeV, 600 GeV, 800 GeV and 1 TeV, all assuming $\sqrt{s} = 14$ TeV and 10 fb^{-1} of integrated luminosity. The starred entries have significance less than 2 and are not included in the summed significance. The double-starred entries have fewer than 2 events in the signal, and are also not included in the total significance.

As Table II shows, the most significant channel(s) vary with the mass of the top-partner. When the top-partner is light, the cross section is large, but the boost of a Higgs or top from T decay is smaller. Consequently, channels which require several substructure tags (Ch. 3, 5) are inefficient, while the high cross section makes up for small branching ratios in the multi-lepton channels (Ch. 2, 4). At high mass, the channels swap roles; the multi-lepton

---

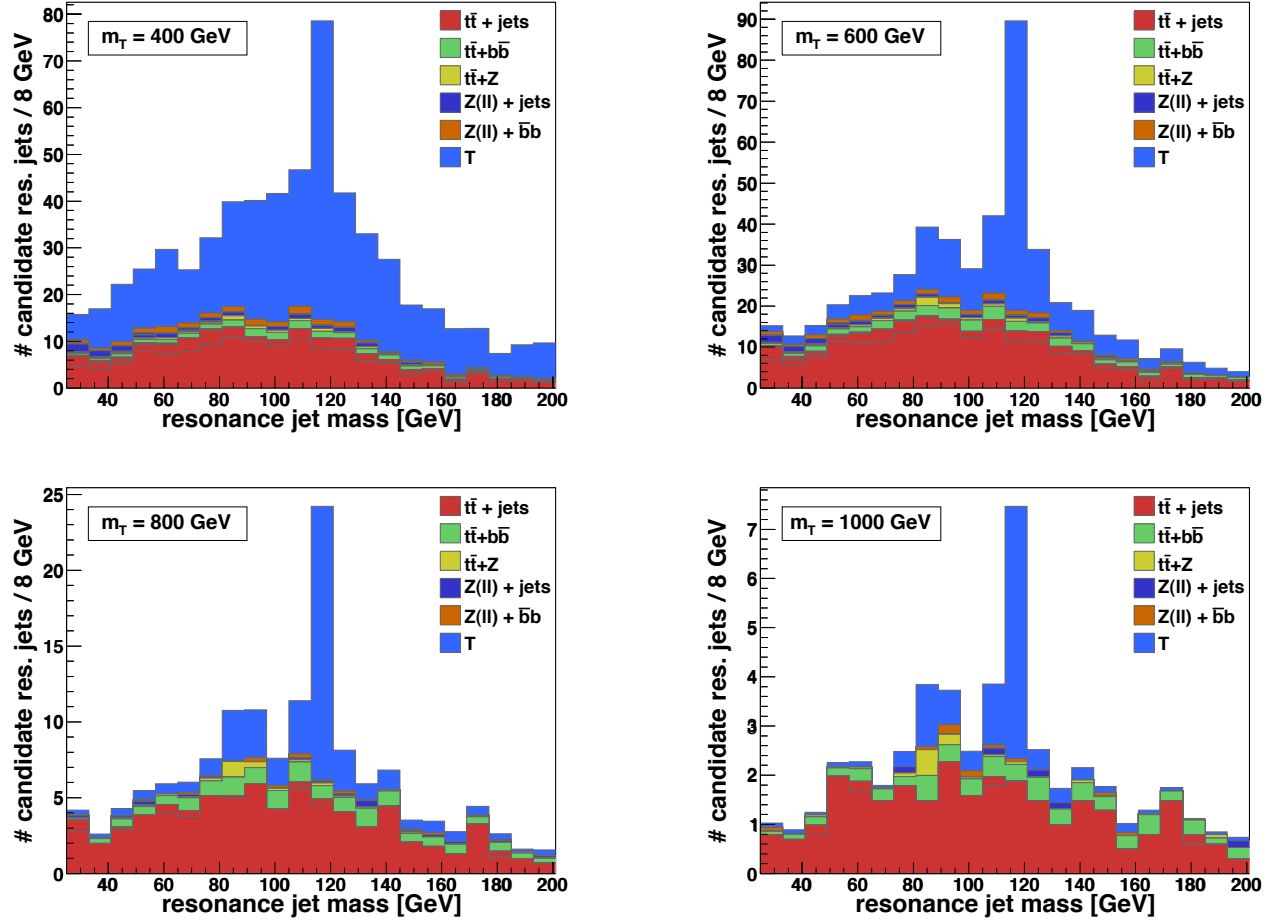[2] and, to a lesser extent, from hadronically decaying Ws as well.

FIG. 7. Resonance jet mass distribution. We assume an integrated luminosity of 10 fb^{-1} at a 14 TeV center of mass LHC. The search strategy is described in Sec. III B and in Fig. 6. An additional cut on $H_T > 1, 1.3$ TeV is imposed for top-partner masses of $800, 1000$ GeV.

channels don't receive enough events, while the efficiency of substructure taggers improves greatly. For the intermediate point, $m_T = 600$ GeV all channels are equally effective.

V. TOP-PARTNERS IN SPECIFIC MODELS

Vector-like top-partners are self-contained extensions of the standard model. Nevertheless, they often appear as ingredients in larger extensions. Here we demonstrate how our results from previous sections on jet substructure and Higgs-finding apply directly to two general classes of models: little Higgs theories and topcolor theories. In particular, we map our parameter space onto two specific examples of these models: the simplest little Higgs model [13] and the top quark seesaw theory of electroweak symmetry breaking [78].

A. The Simplest Little Higgs

In the simplest little Higgs model, the Higgs boson is naturally light because it is a Nambu-Goldstone boson of a spontaneously broken symmetry $(\mathrm{SU}(3)_W \times U(1)_X)/(\mathrm{SU}(2)_W \times U(1)_Y)$. Nonzero vevs of two scalars (say, ϕ_1 and ϕ_2) in the triplet representation of $\mathrm{SU}(3)_W$ break the full symmetry down to $\mathrm{SU}(2)_W \times U(1)_Y$ at the scale $f > v$. Interactions of SM Higgs doublet can easily be calculated in the following parametrization of the ϕ_i fields:

$$\phi_1 = \exp\left\{ i \begin{pmatrix} & H^\dagger \\ H & \end{pmatrix} \right\} \begin{pmatrix} \\ f \end{pmatrix} \tag{9}$$

$$\phi_2 = \exp\left\{ -i \begin{pmatrix} & H^\dagger \\ H & \end{pmatrix} \right\} \begin{pmatrix} \\ f \end{pmatrix} \tag{10}$$

The quadratic divergences associated with the top Yukawa is cancelled by extending the SU(3) symmetry

to the Yukawa couplings. First, the quark doublets are enlarged into $SU(3)$ triplets: $\Psi \equiv (Q_3, T)$, transforming under the $SU(3)_W$ gauge symmetry. Second, two color-triplet, $SU(3)_W$-singlets T_1^c and T_2^c are introduced. The $U(1)_X$ charges of T_1^c and T_2^c are chosen to be equal and identical to the $U(1)_X$ charge of t^c.

$$\mathcal{L}_{\text{Yukawa}} = \lambda_1 \phi_1^\dagger \Psi T_1^c + \lambda_2 \phi_2^\dagger \Psi T_2^c \,. \tag{11}$$

Expanding ϕ_1 and ϕ_2 around their vevs (as in Eq. (9)) we find the effective Lagrangian

$$\mathcal{L} \supset HQ_3 \left(\lambda_1 T_1^c - \lambda_2 T_2^c\right)$$
$$+ fT \left(\lambda_1 T_1^c + \lambda_2 T_2^c\right) \left(1 - \frac{1}{2f^2} H^\dagger H\right) + \dots \,. \tag{12}$$

The above set of interactions can be recast in the form of Eq. (1) by the following substitutions

$$t_c = \frac{1}{\sqrt{\lambda_1^2 + \lambda_2^2}} \left(\lambda_1 T_1^c - \lambda_2 T_2^c\right)$$

$$T_c = \frac{1}{\sqrt{\lambda_1^2 + \lambda_2^2}} \left(\lambda_2 T_1^c + \lambda_1 T_2^c\right)$$

$$y_1 = \sqrt{\lambda_1^2 + \lambda_2^2}$$

$$\delta = \frac{\lambda_1^2 - \lambda_2^2}{\sqrt{\lambda_1^2 + \lambda_2^2}} f \,, \quad M = \frac{2\lambda_1 \lambda_2}{\sqrt{\lambda_1^2 + \lambda_2^2}} f \,.$$

B. Top quark seesaw theory

In topcolor models, the Higgs boson is a composite particle formed from top quarks and new, heavier fermions as the result of some TeV-scale strong dynamics. In the top quark seesaw theory [78], the gauge structure is enlarged to $SU(3)_1 \times SU(3)_2 \times SU(2)_W \times U(1)_Y$. The third generation of SM quarks, along with an additional pair of quarks, are embedded as

$$Q'(\mathbf{3}, \mathbf{1}, \mathbf{2}, 1/6), \quad T'(\mathbf{3}, \mathbf{1}, \mathbf{1}, +2/3),$$
$$T'^c(\mathbf{1}, \bar{\mathbf{3}}, \mathbf{1}, -2/3), \quad t'^c(\mathbf{1}, \bar{\mathbf{3}}, \mathbf{1}, -2/3).$$

Topcolor is broken to QCD, $SU(3)_1 \times SU(3)_2 \to SU(3)_C$, through a scalar link field transforming as a $(\bar{\mathbf{3}}, \mathbf{3}, \mathbf{1}, 0)$. This results in a composite Higgs doublet formed from a bound state of Q' with t'^c. The low energy effective theory is just the SM group with an additional pair of quarks that transform under a vector-like representation as well as a color octet of massive gauge bosons. Below the scale of the color octet, the theory contains the identical particle content and interactions given by Eq. (1).

Translating Ref. [78] into the notation presented here requires the fields be relabeled as

$$t_L \to t_L$$
$$\chi_L \to T$$
$$t_R \to T^{c*}$$
$$\chi_R \to t^{c*},$$

and the mass terms relabeled as

$$m_{t\chi} \to m$$
$$\mu_{\chi t} \to M$$
$$\mu_{\chi\chi} \to \delta.$$

This "schematic model" involving only one composite Higgs boson has a large Higgs mass, $\mathcal{O}(1 \text{ TeV})$. However, as emphasized by Ref. [78], a more general theory of the the seesaw mechanism for electroweak symmetry breaking involves more composite scalars, allowing one of the neutral Higgs bosons to be as light as $\mathcal{O}(100 \text{ GeV})$.

One example of a more general topcolor theory involves extra dimensions [23]. In the extra dimensional form, a strongly interacting top quark is described by promoting the right-handed top into a 5D bulk fermion and giving it a profile which overlaps with the strong sector. Reduced to a 4D theory, the KK modes of t_R become fermionic resonances, more massive copies of t_R with exactly the quantum numbers of the top-partner we are studying. Boundary conditions slightly mix the various t_R modes. When truncated to the zero modes of t_L, t_R and the first t_R KK excitation, the top quark mass matrix has exactly the form of our Eq. (2). Other extra dimensional models can be found in Ref. [24–26] and deconstructed versions in Ref. [79].

VI. DISCUSSION

We have demonstrated that top-partner production and decay leads to highly boosted, light Higgs bosons that can be discovered in their dominant $b\bar{b}$ decay mode through the use of jet substructure techniques. For top-parters with masses in the range $400 - 800$ GeV, we explicitly showed that our estimate of the $S/\sqrt{B}$ of Higgs discovery exceeds 5 with just 10 fb^{-1} of 14 TeV LHC data. This is all the more remarkable given that top-partner decay results in just SM particles in the final state. We demonstrated that a multi-channel analysis yields the best approach to maximizing Higgs boson discovery significance. Our analysis thus explicitly demonstrates the full extent of our original observation in 2009 [62] that Higgs production and decay to $b\bar{b}$ through new physics production may well be *the* discovery mode of the Higgs boson. Finally, the methods we employed in the paper to find the Higgs boson can also be applied as additional search channels for top-partner production itself. Comparing the significance of our channels against older studies [40, 41] suggests that including the Higgs boson in the final state may well accelerate the discovery of top-partners!

It is interesting to compare and constrast top-partner production and decay against the superpartner production and decay to Higgs bosons. One of the main ingredients of [62, 63] was to isolate the supersymmetric signal from SM backgrounds using large missing energy, which resulted from the escaping lightest supersymmetric partners. Top-partner production and decay, by constrast,

always results in just SM particles in the final state. The reason top-partner production is *viable* is mainly because of the large fraction of top-partner decays that contain a substantially boosted Higgs boson. We demonstrated (*c.f.* Fig. 5) that the Higgs boson p_T peaks at roughly $m_T/2$, whereas the Higgs boson typically receives less of a boost in a supersymmetric cascade, $\mathcal{O}(m_{\tilde{q}}/4)$, and thus requires more massive squarks, which lowers the production cross section. In supersymmetry, this is partially compensated by the potentially large number of squark production channels that could lead to Higgs bosons in the final state [63].

Finally, while we have focused on the top-partner in isolation, there are many models for which it is but one component of a larger extension beyond the standard model. We explicitly demonstrated that the particle content and interactions arise precisely in the simplest little Higgs model [13] as well as the top quark seesaw model of electroweak symmetry breaking [78]. These are but two examples of a large class of models where, if the Higgs boson is light enough, it can be discovered through new physics production and decay. The case of topcolor models is particularly interesting, since they also have a massive color-octet vector boson that couples to (light and heavy) quarks, potentially dramatically increasing the production cross section of top partners if the color-octet is not too heavy [64]. Bottom-partners also provide an interesting accompanying particles that can result in Higgs bosons. However, since bottom-partners could decay to bh, bZ and Wt, in complete analogy to T, they can pollute T events making the extraction of the Higgs boson harder. However, a nearly degenerate bottom-partner can also provide great Higgs discovery opportunities on its own. More elaborate vector-like extensions of the SM also exist where the branching fraction to $h+X$ can increase dramatically to even 100% [80] making this analysis even more significant. However, the extreme branching fractions require special combinations of field content and mixing angles.

Appendix: Background details

In Table III we summarize all the background events we have considered in this work. We list their cross sections along with the the parton-level cuts we use to generate these events. To avoid over-counting in the $\bar{t}t+$ jets and $W/Z+$ jets backgrounds, MLM jet-parton matching was performed according to the procedure outlined in [81–83].

Process	σ_{LHC}
$\bar{t}t + 0$ jets	254 pb
$\bar{t}t + 1$ jets	133 pb
$\bar{t}t + 2^+$ jets	71 pb
$\bar{t}t + \bar{b}b$	2.6 pb
$\bar{t}t + Z$	1.1 pb
$Z(\ell\ell) + 2$ jets	80 pb
$Z(\ell\ell) + 3^+$ jets	29 pb
$Z(\ell\ell) + \bar{b}b$	82 pb
$Z(\ell\ell) + \bar{b}b + $ jet	31 pb

TABLE III. Background cross sections at a $\sqrt{s} = 14$ TeV center of mass LHC. CTEQ5L pdfs and default renormalization and factorization scales were used for all background processes. Parton level cuts of $p_{T,j} > 25$ GeV, $|\eta_j| < 4, \Delta R_{jj} > 0.4$ were applied when generating all events with the exception that no p_T or $|\eta|$ requirements were placed on the b-jets from $W/Z + \bar{b}b$. The $\bar{t}t+$jets, $\bar{t}t + \bar{b}b$ and $\bar{t}t + Z$ cross sections have all been scaled to NLO using K factors taken from [55, 84–88].

In addition to the above backgrounds, we checked $W + 2, 3$ jets and $W + \bar{b}b + 0, 1$ jets. These processes, especially $W +$ jets, have large cross sections, but they fall mostly within the 1 lepton, 0-top channel. By requiring an extra b-jet and an extra tagged W/Z these backgrounds can be successfully mitigated. We find they comprise a few percent, at most of the background above, so we do not include them in our analysis.

[1] N. Arkani-Hamed, A. G. Cohen, and H. Georgi, Phys. Lett. **B513**, 232 (2001), arXiv:hep-ph/0105239.

[2] N. Arkani-Hamed, A. Cohen, E. Katz, A. Nelson, T. Gregoire, *et al.*, JHEP **0208**, 021 (2002), arXiv:hep-ph/0206020 [hep-ph].

[3] N. Arkani-Hamed, A. Cohen, E. Katz, and A. Nelson, JHEP **0207**, 034 (2002), arXiv:hep-ph/0206021 [hep-ph].

[4] I. Low, W. Skiba, and D. Tucker-Smith, Phys.Rev. **D66**, 072001 (2002), arXiv:hep-ph/0207243 [hep-ph].

[5] M. Schmaltz, Nucl. Phys. Proc. Suppl. **117**, 40 (2003), arXiv:hep-ph/0210415.

[6] D. E. Kaplan and M. Schmaltz, JHEP **10**, 039 (2003), arXiv:hep-ph/0302049.

[7] W. Skiba and J. Terning, Phys. Rev. **D68**, 075001 (2003), arXiv:hep-ph/0305302.

[8] S. Chang and J. G. Wacker, Phys. Rev. **D69**, 035002

(2004), arXiv:hep-ph/0303001.

[9] S. Chang, JHEP **12**, 057 (2003), arXiv:hep-ph/0306034.

[10] H.-C. Cheng and I. Low, JHEP **09**, 051 (2003), arXiv:hep-ph/0308199.

[11] E. Katz, J.-y. Lee, A. E. Nelson, and D. G. E. Walker, JHEP **10**, 088 (2005), arXiv:hep-ph/0312287.

[12] H.-C. Cheng and I. Low, JHEP **08**, 061 (2004), arXiv:hep-ph/0405243.

[13] M. Schmaltz, JHEP **0408**, 056 (2004), arXiv:hep-ph/0407143 [hep-ph].

[14] I. Low, JHEP **10**, 067 (2004), arXiv:hep-ph/0409025.

[15] C. Csaki, J. Hubisz, G. D. Kribs, P. Meade, and J. Terning, Phys. Rev. **D67**, 115002 (2003), arXiv:hep-ph/0211124.

[16] J. L. Hewett, F. J. Petriello, and T. G. Rizzo, JHEP **10**, 062 (2003), arXiv:hep-ph/0211218.

[17] C. Csaki, J. Hubisz, G. D. Kribs, P. Meade, and J. Terning, Phys. Rev. **D68**, 035009 (2003), arXiv:hep-ph/0303236.

[18] M.-C. Chen and S. Dawson, Phys. Rev. **D70**, 015003 (2004), arXiv:hep-ph/0311032.

[19] G. Burdman, M. Perelstein, and A. Pierce, Phys. Rev. Lett. **90**, 241802 (2003), arXiv:hep-ph/0212228.

[20] T. Han, H. E. Logan, B. McElrath, and L.-T. Wang, Phys.Rev. **D67**, 095004 (2003), arXiv:hep-ph/0301040 [hep-ph].

[21] M. Perelstein, M. E. Peskin, and A. Pierce, Phys. Rev. **D69**, 075002 (2004), arXiv:hep-ph/0310039.

[22] H.-C. Cheng, I. Low, and L.-T. Wang, Phys. Rev. **D74**, 055001 (2006), arXiv:hep-ph/0510225.

[23] H.-C. Cheng, B. A. Dobrescu, and C. T. Hill, Nucl.Phys. **B589**, 249 (2000), arXiv:hep-ph/9912343 [hep-ph].

[24] M. S. Carena, E. Ponton, J. Santiago, and C. E. Wagner, Nucl.Phys. **B759**, 202 (2006), arXiv:hep-ph/0607106 [hep-ph].

[25] R. Contino, L. Da Rold, and A. Pomarol, Phys.Rev. **D75**, 055014 (2007), arXiv:hep-ph/0612048 [hep-ph].

[26] G. Burdman and L. Da Rold, JHEP **0712**, 086 (2007), arXiv:0710.0623 [hep-ph].

[27] C. T. Hill, Phys. Lett. **B266**, 419 (1991).

[28] A. Birkedal, Z. Chacko, and M. K. Gaillard, JHEP **10**, 036 (2004), arXiv:hep-ph/0404197.

[29] P. H. Chankowski, A. Falkowski, S. Pokorski, and J. Wagner, Phys. Lett. **B598**, 252 (2004), arXiv:hep-ph/0407242.

[30] Z. Chacko, Y. Nomura, and D. Tucker-Smith, Nucl. Phys. **B725**, 207 (2005), arXiv:hep-ph/0504095.

[31] T. S. Roy and M. Schmaltz, JHEP **01**, 149 (2006), arXiv:hep-ph/0509357.

[32] C. Csaki, G. Marandella, Y. Shirman, and A. Strumia, Phys. Rev. **D73**, 035006 (2006), arXiv:hep-ph/0510294.

[33] A. Falkowski, S. Pokorski, and M. Schmaltz, Phys. Rev. **D74**, 035003 (2006), arXiv:hep-ph/0604066.

[34] S. Chang, L. J. Hall, and N. Weiner, Phys. Rev. **D75**, 035009 (2007), arXiv:hep-ph/0604076.

[35] B. Bellazzini, C. Csaki, A. Delgado, and A. Weiler, Phys. Rev. **D79**, 095003 (2009), arXiv:0902.0015 [hep-ph].

[36] C. Kilic, K. Kopp, and T. Okui, (2010), arXiv:1008.2763 [hep-ph].

[37] G. Azuelos, K. Benslama, D. Costanzo, G. Couture, J. Garcia, *et al.*, Eur.Phys.J. **C39S2**, 13 (2005), arXiv:hep-ph/0402037 [hep-ph].

[38] K. Karafasoulis, A. Kyriakis, H. Petrakou, and K. Mazumdar, *Little Higgs Model and Top-like Heavy Quark at CMS*, Tech. Rep. CMS-NOTE-2006-079. CERN-CMS-NOTE-2006-079 (CERN, Geneva, 2006).

[39] S. Matsumoto, M. M. Nojiri, and D. Nomura, Phys. Rev. **D75**, 055006 (2007), arXiv:hep-ph/0612249.

[40] W. Skiba and D. Tucker-Smith, Phys.Rev. **D75**, 115010 (2007), arXiv:hep-ph/0701247 [hep-ph].

[41] B. Holdom, JHEP **03**, 063 (2007), arXiv:hep-ph/0702037.

[42] B. Holdom, JHEP **08**, 069 (2007), arXiv:0705.1736 [hep-ph].

[43] T. Aaltonen *et al.* (CDF Collaboration), Phys.Rev.Lett. **100**, 161803 (2008), arXiv:0801.3877 [hep-ex].

[44] A. Lister (CDF Collaboration), (2008), arXiv:0810.3349 [hep-ex].

[45] J. A. Aguilar-Saavedra, JHEP **11**, 030 (2009), arXiv:0907.3155 [hep-ph].

[46] J. M. Butterworth, A. R. Davison, M. Rubin, and G. P. Salam, Phys.Rev.Lett. **100**, 242001 (2008), arXiv:arXiv:0802.2470 [hep-ph].

[47] J. Butterworth, B. Cox, and J. R. Forshaw, Phys.Rev. **D65**, 096014 (2002), arXiv:hep-ph/0201098 [hep-ph].

[48] J. Thaler and L.-T. Wang, JHEP **07**, 092 (2008), arXiv:0806.0023 [hep-ph].

[49] G. H. Brooijmans, A. Delgado, B. A. Dobrescu, C. Grojean, M. Narain, *et al.*, , 363 (2008), arXiv:arXiv:0802.3715 [hep-ph].

[50] L. G. Almeida *et al.*, Phys. Rev. **D79**, 074017 (2009), arXiv:0807.0234 [hep-ph].

[51] L. G. Almeida, S. J. Lee, G. Perez, I. Sung, and J. Virzi, Phys. Rev. **D79**, 074012 (2009), arXiv:0810.0934 [hep-ph].

[52] J. M. Butterworth, J. R. Ellis, A. R. Raklev, and G. P. Salam, Phys.Rev.Lett. **103**, 241803 (2009), arXiv:arXiv:0906.0728 [hep-ph].

[53] S. D. Ellis, C. K. Vermilion, and J. R. Walsh, Phys.Rev. **D80**, 051501 (2009), arXiv:arXiv:0903.5081 [hep-ph].

[54] S. D. Ellis, C. K. Vermilion, and J. R. Walsh, Phys. Rev. **D81**, 094023 (2010), arXiv:0912.0033 [hep-ph].

[55] T. Plehn, G. P. Salam, and M. Spannowsky, Phys.Rev.Lett. **104**, 111801 (2010), arXiv:arXiv:0910.5472 [hep-ph].

[56] D. Krohn, J. Thaler, and L.-T. Wang, JHEP **0906**, 059 (2009), arXiv:arXiv:0903.0392 [hep-ph].

[57] D. Krohn, J. Thaler, and L.-T. Wang, JHEP **02**, 084 (2010), arXiv:0912.1342 [hep-ph].

[58] S. Chekanov and J. Proudfoot, Phys.Rev. **D81**, 114038 (2010), arXiv:arXiv:1002.3982 [hep-ph].

[59] D. E. Soper and M. Spannowsky, JHEP **1008**, 029 (2010), arXiv:arXiv:1005.0417 [hep-ph].

[60] C. Hackstein and M. Spannowsky, (2010), arXiv:arXiv:1008.2202 [hep-ph].

[61] A. Katz, M. Son, and B. Tweedie, (2010), arXiv:arXiv:1010.5253 [hep-ph].

[62] G. D. Kribs, A. Martin, T. S. Roy, and M. Spannowsky, Phys.Rev. **D81**, 111501 (2010), arXiv:arXiv:0912.4731 [hep-ph].

[63] G. D. Kribs, A. Martin, T. S. Roy, and M. Spannowsky, (2010), arXiv:arXiv:1006.1656 [hep-ph].

[64] B. A. Dobrescu, K. Kong, and R. Mahbubani, JHEP **0906**, 001 (2009), arXiv:arXiv:0902.0792 [hep-ph].

[65] D. E. Kaplan, K. Rehermann, M. D. Schwartz, and B. Tweedie, Phys.Rev.Lett. **101**, 142001 (2008), arXiv:arXiv:0806.0848 [hep-ph].

[66] T. Plehn, M. Spannowsky, M. Takeuchi, and D. Zerwas,

(2010), arXiv:1006.2833 [hep-ph].

[67] M. Spannowsky, (2010), talk given at University of Oregon & University of Washington workshop on 'The Terascale at LHC 0.5 and Tevatron'.

[68] Y. L. Dokshitzer, G. D. Leder, S. Moretti, and B. R. Webber, JHEP **08**, 001 (1997), arXiv:hep-ph/9707323.

[69] M. Wobisch and T. Wengler, (1998), arXiv:hep-ph/9907280.

[70] M. Wobisch, (2000), DESY-THESIS-2000-049.

[71] *ATLAS Sensitivity to the Standard Model Higgs in the HW and HZ Channels at High Transverse Momenta*, Tech. Rep. ATL-PHYS-PUB-2009-088 (CERN, Geneva, 2009).

[72] F. Maltoni and T. Stelzer, JHEP **02**, 027 (2003), hep-ph/0208156.

[73] J. Alwall *et al.*, JHEP **09**, 028 (2007), arXiv:0706.2334 [hep-ph].

[74] T. Sjostrand, S. Mrenna, and P. Skands, JHEP **05**, 026 (2006), hep-ph/0603175.

[75] C. M. Buttar, D. Clements, I. Dawson, and A. Moraes, Acta Phys. Polon. **B35**, 433 (2004).

[76] M. L. Mangano, M. Moretti, F. Piccinini, R. Pittau, and A. D. Polosa, JHEP **07**, 001 (2003), hep-ph/0206293.

[77] M. Cacciari and G. P. Salam, Phys. Lett. **B641**, 57 (2006), arXiv:hep-ph/0512210.

[78] R. Chivukula, B. A. Dobrescu, H. Georgi, and C. T. Hill, Phys.Rev. **D59**, 075003 (1999), arXiv:hep-ph/9809470 [hep-ph].

[79] R. Sekhar Chivukula, N. D. Christensen, B. Coleppa, and E. H. Simmons, Phys.Rev. **D80**, 035011 (2009), arXiv:0906.5567 [hep-ph].

[80] S. P. Martin, Phys.Rev. **D81**, 035004 (2010), arXiv:arXiv:0910.2732 [hep-ph].

[81] M. Mangano, (2004), http://mlm.web.cern.ch/mlm/talks/lund-alpgen.pdf.

[82] S. Catani, F. Krauss, R. Kuhn, and B. R. Webber, JHEP **11**, 063 (2001), arXiv:hep-ph/0109231.

[83] J. Alwall *et al.*, Eur. Phys. J. **C53**, 473 (2008), arXiv:0706.2569 [hep-ph].

[84] G. Bevilacqua, M. Czakon, C. Papadopoulos, and M. Worek, Phys.Rev.Lett. **104**, 162002 (2010), arXiv:1002.4009 [hep-ph].

[85] S. Dittmaier, P. Uwer, and S. Weinzierl, Eur.Phys.J. **C59**, 625 (2009), arXiv:0810.0452 [hep-ph].

[86] G. Bevilacqua, M. Czakon, C. Papadopoulos, R. Pittau, and M. Worek, JHEP **0909**, 109 (2009), arXiv:0907.4723 [hep-ph].

[87] A. Bredenstein, A. Denner, S. Dittmaier, and S. Pozzorini, Phys.Rev.Lett. **103**, 012002 (2009), arXiv:0905.0110 [hep-ph].

[88] A. Lazopoulos, T. McElmurry, K. Melnikov, and F. Petriello, Phys.Lett. **B666**, 62 (2008), arXiv:0804.2220 [hep-ph].